

LIST OF CONTENTS

Supplementary Figures

Figure S1. LuxN antagonist potencies.

Figure S2. Ligand specificity when LuxN is produced from a plasmid.

Figure S3. LuxN mutants with broadened ligand specificity.

Figure S4. The LuxN^{L166R} variant shows no response to AHLs.

Figure S5. The AinR variants' responses to AHLs.

Figure S6. The LuxN Kin^{off} mutants are not null mutants.

Figure S7. LuxN mutants display a spectrum of biases to the Kin^{off} state.

Supplementary Tables

Table S1. LuxN and LuxN His210 variants' sensitivities to AHLs with different C₃ modifications.

Table S2. LuxN, LuxN His210, LuxN Leu166 variants' sensitivities to AHLs.

Table S3. AinR receptors' sensitivities to AHLs.

Table S4. LuxN Kin^{off} receptors' sensitivities to 3O-C12 HSL.

Supplementary Experimental Procedures

Supplementary References

¹H NMR Spectra

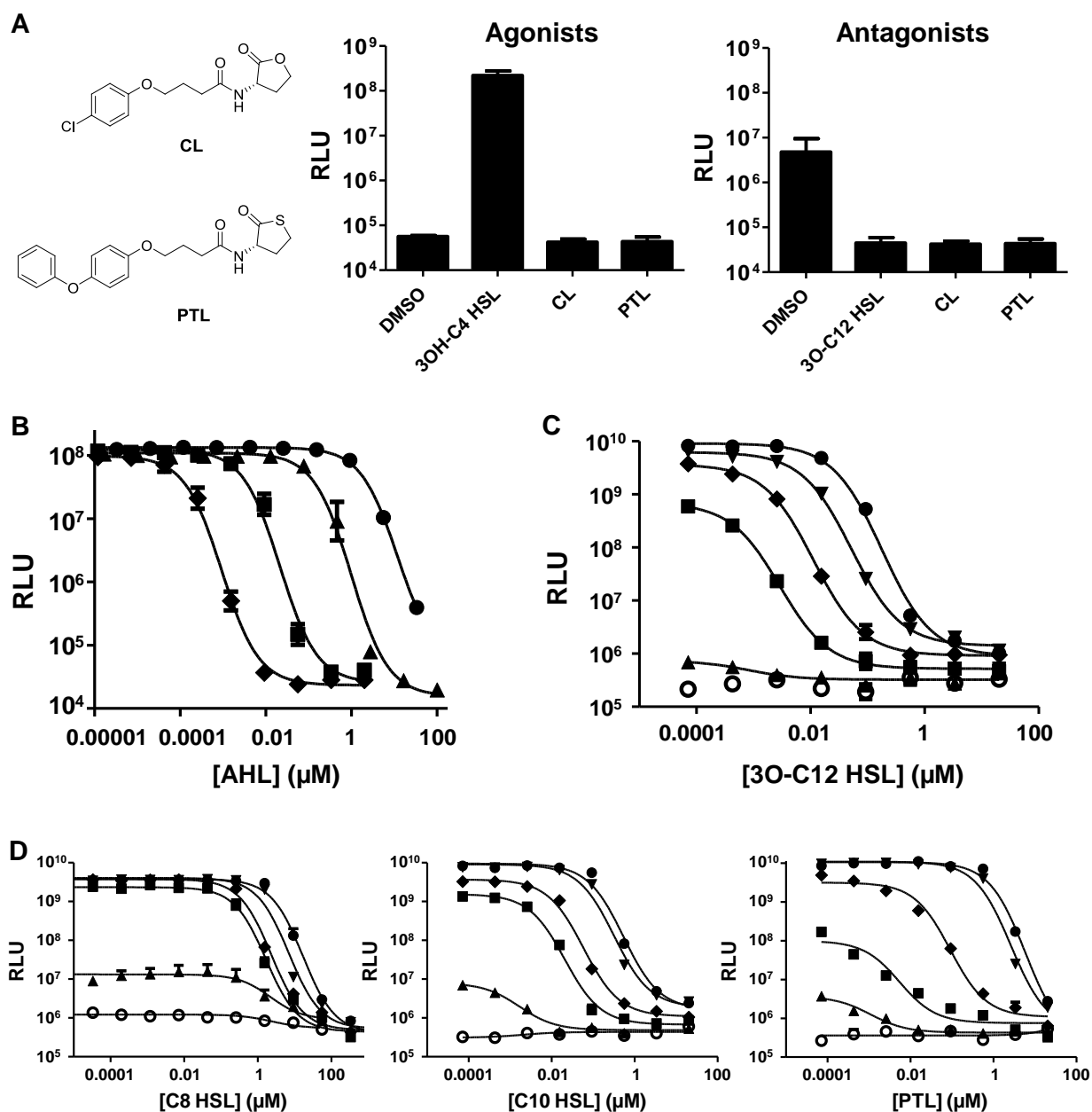


Figure S1. LuxN antagonist potencies.

(A) Light production from *V. harveyi* TL25 was measured in response to the specified compounds supplied at 1 μM as in Fig 1. Structures of CL and PTL are shown on the left for reference. In the antagonist assay (right panel), 20 nM AI-1 was provided along with the specified compounds.

(B) Dose-dependent light production from *V. harveyi* TL25 was measured with antagonists supplied at the concentrations specified on the x-axis along with 20 nM AI-1. C6-HSL, circles; C8-HSL, triangles; C10-HSL, squares; C12 HSL, diamonds. Error bars represent standard deviations for three replicates.

(C) Antagonism of the LuxN/AI-1 interaction by 3O-C12 HSL at the concentrations specified on the X-axis. The following concentrations of AI-1 were provided: none, open circles; 5 nM, triangles; 20 nM, squares; 50 nM, diamonds; 200 nM, inverted triangles; 500 nM, closed circles.

(D) LuxN antagonism by C8 HSL, C10 HSL, and PTL. Bioluminescence assays were performed as in C.

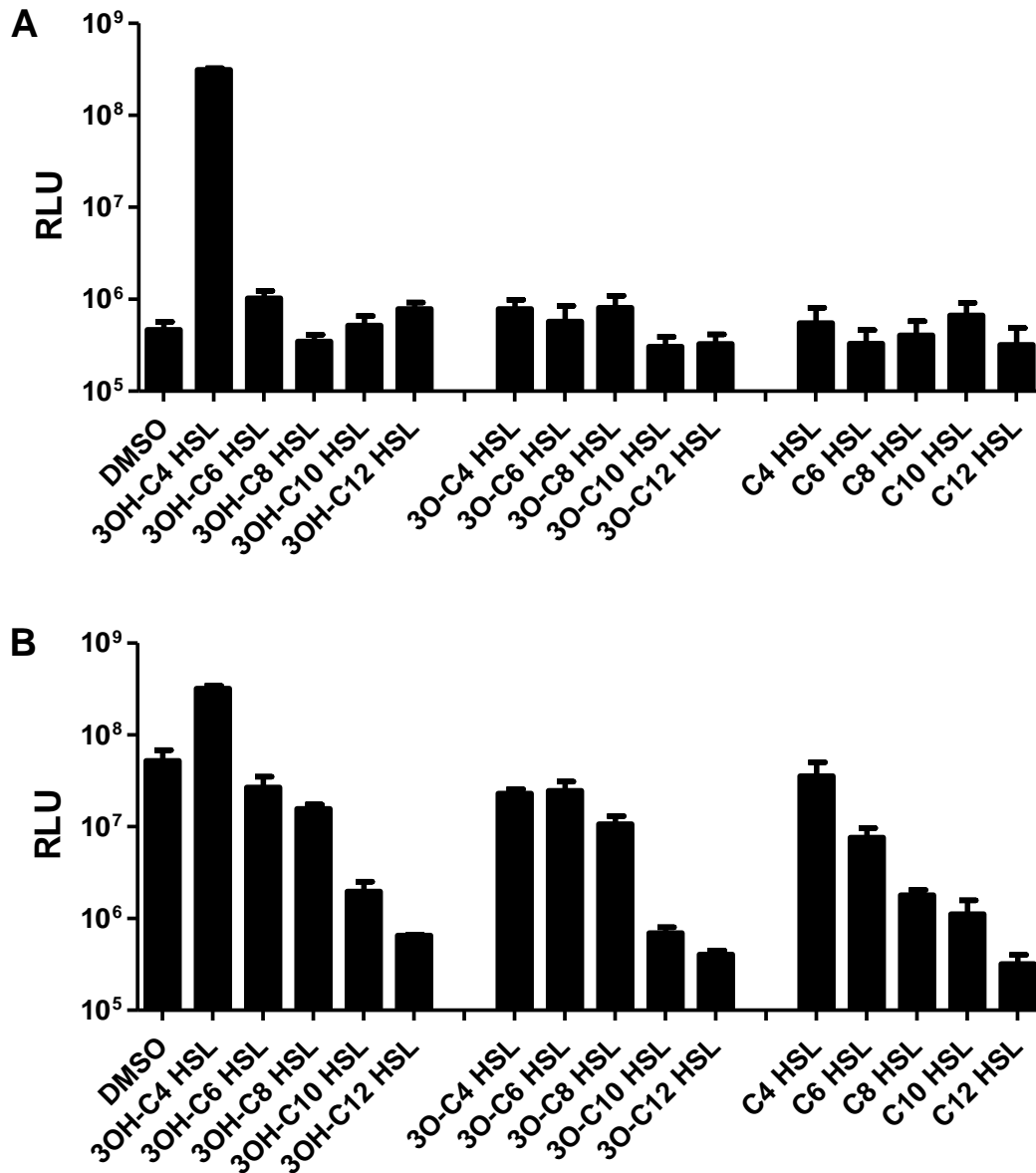


Figure S2. Ligand specificity when LuxN is produced from a plasmid.

(A) Light production in response to the specified AHLs at 1 μ M concentration was measured for *V. harveyi* XK006 carrying WT *luxN*.

(B) Antagonist assays were performed as in Fig. 1. Error bars represent standard deviations for three replicates.

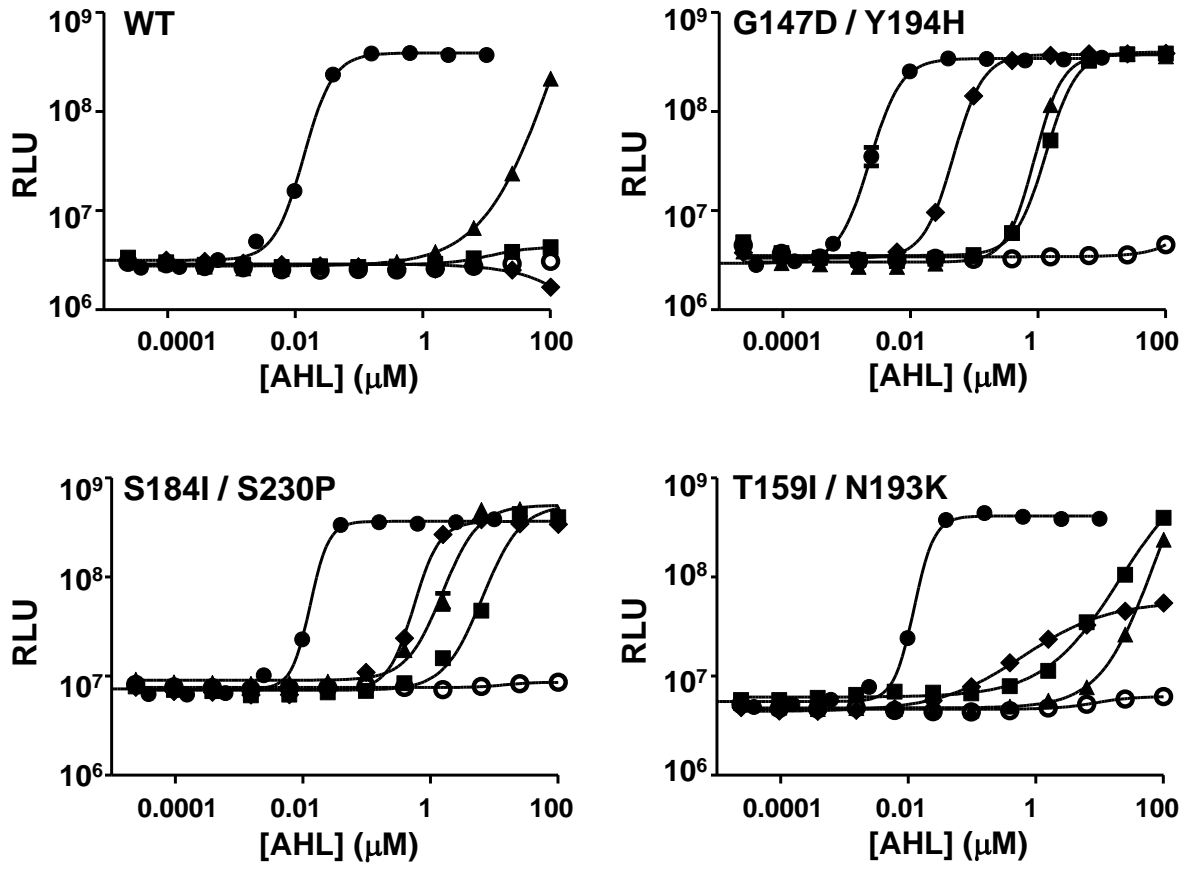


Figure S3. LuxN mutants with broadened ligand specificity.

Dose-dependent responses of *V. harveyi* XK006 carrying WT *luxN* or the specified *luxN* alleles (DMSO, open circles; AI-1 (3OH-C4 HSL), closed circles; C4 HSL, triangles; 3O-C8 HSL, squares; 3O-C10 HSL, diamonds).

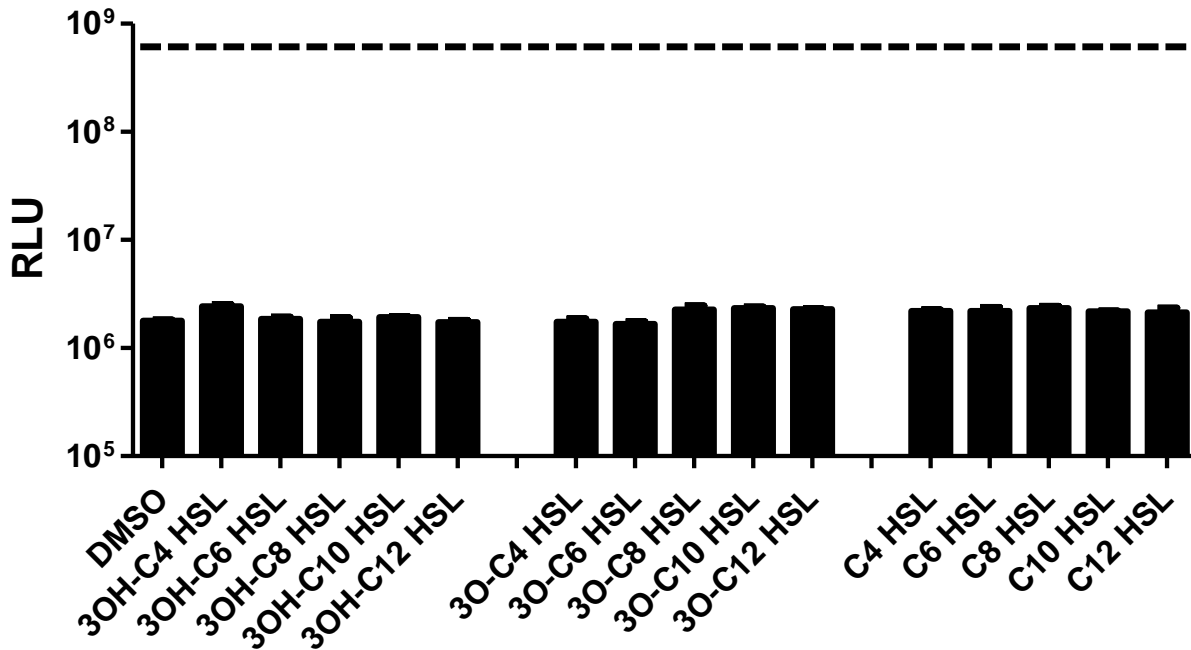


Figure S4. The LuxN^{L166R} variant shows no response to AHLs.

V. harveyi XK006 carrying *luxN*^{L166R} was assayed for light production in response to the specified AHLs at 1 μM concentration. Error bars represent standard deviations for three replicates. The dashed line represents the maximal level of light produced by *V. harveyi*.

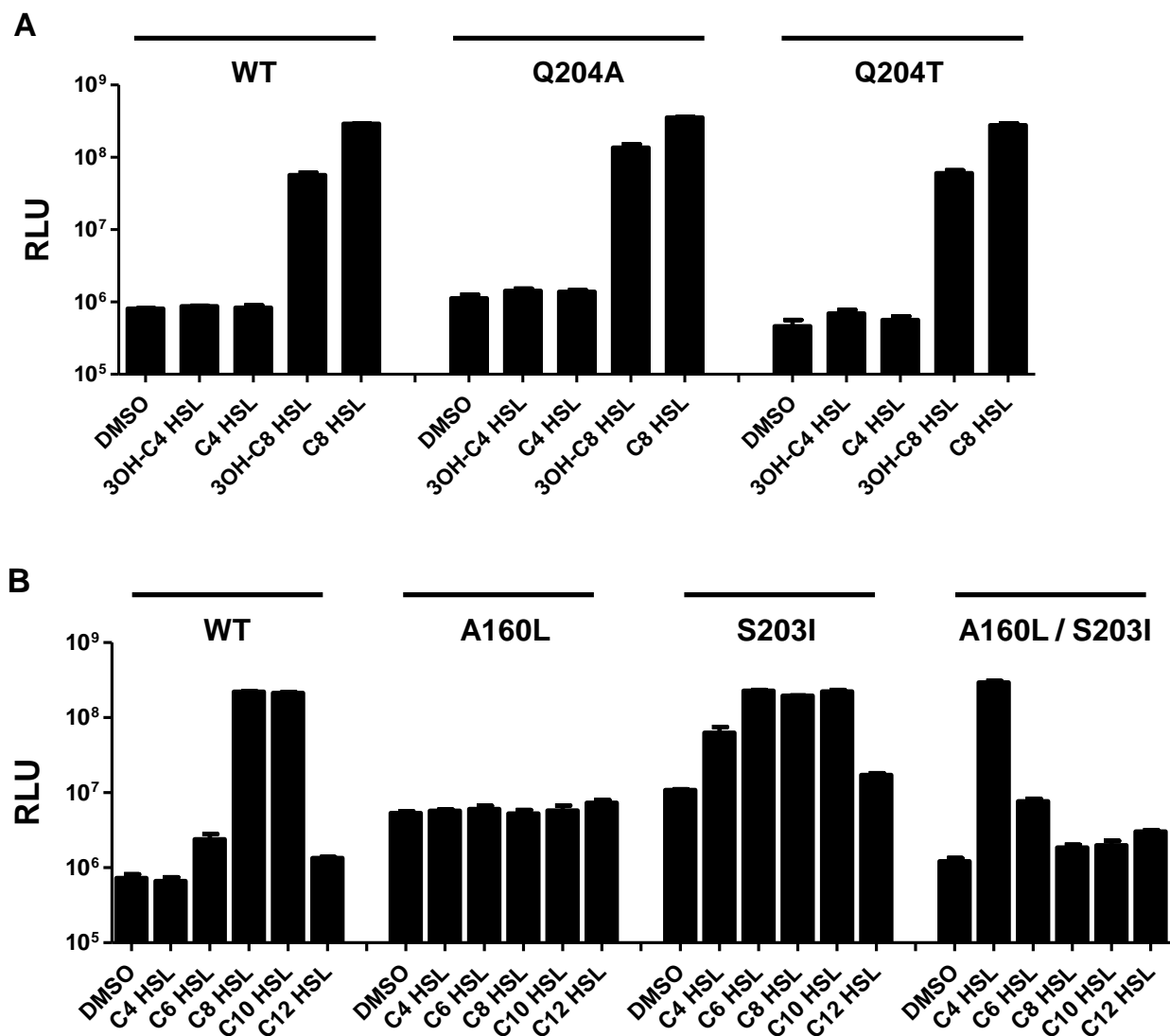


Figure S5. The AinR variants' responses to AHLs.

(A) *V. harveyi* XK006 carrying the designated *ainR* Gln204 alleles was assayed for light production in response to the specified AHLs at 1 μ M concentration. Error bars represent standard deviations for three replicates.

(B) *V. harveyi* XK006 carrying the designated *ainR* alleles was assayed for light production to the specified AHLs. Bioluminescence was measured as in A.

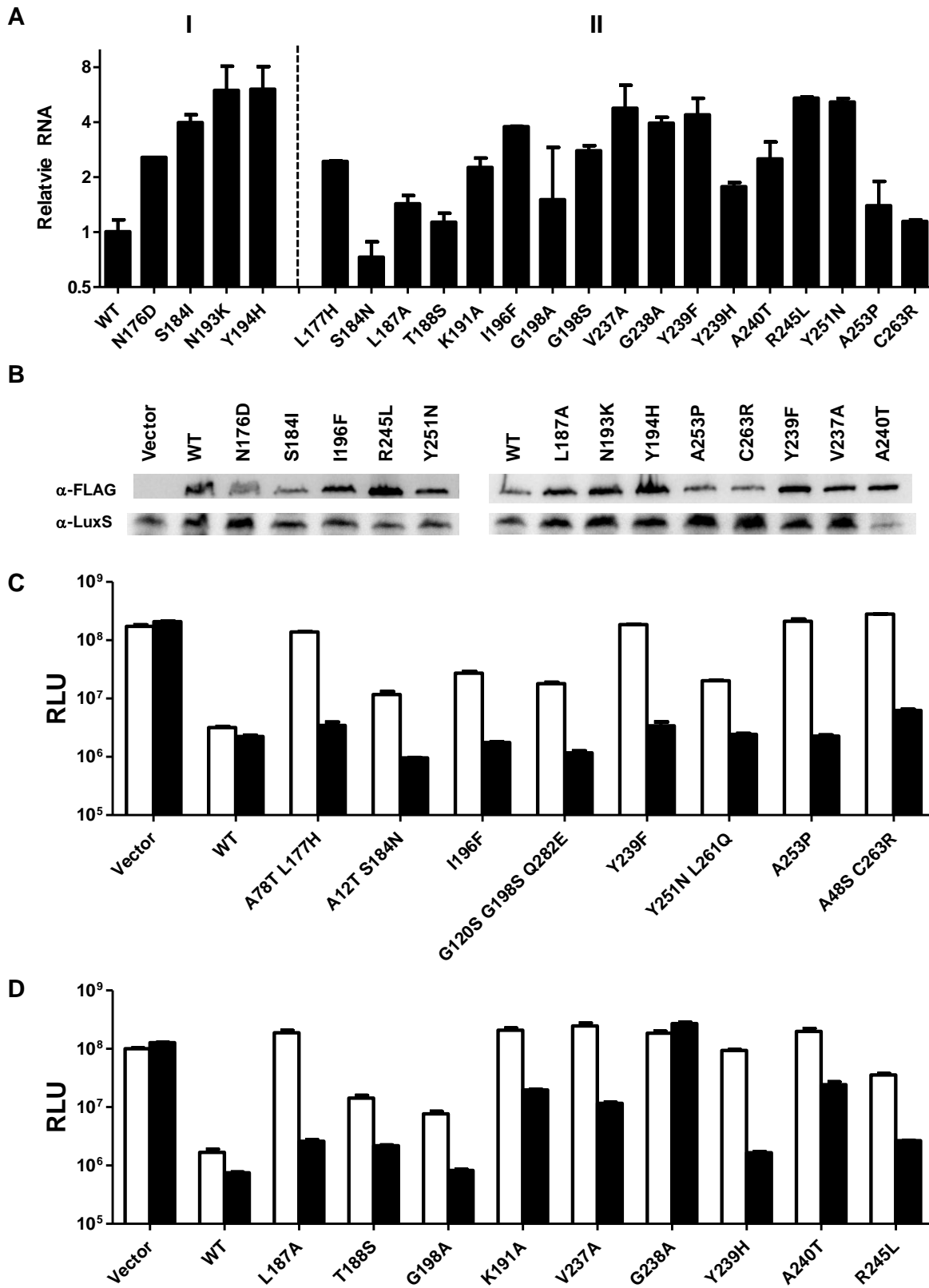


Figure S6

Figure S6. The LuxN Kin^{off} mutants are not null mutants.

(A) *luxN* mRNA levels were measured for *V. harveyi* XK006 carrying WT or Kin^{off} *luxN* alleles by qRT-PCR. *hfq* mRNA was used as the internal control. All *luxN* transcript levels were normalized to that of the WT *luxN*. Error bars represent standard deviations for two replicates. Alleles in panel I refer to Fig. 3 and alleles in panel II are the additional Kin^{off} mutants identified through screening.

(B) Western blot analysis of FLAG tagged LuxN protein detected in whole-cell lysates made from *V. harveyi* XK006 carrying the pFED343 vector, WT *luxN*-FLAG construct, or representative *luxN*-FLAG constructs of Kin^{off} alleles. LuxS protein was used as the loading control.

(C) Bioluminescence phenotypes of *V. harveyi* XK006 carrying the vector, WT *luxN*, or *luxN* alleles isolated from the screen for Kin^{off} LuxN mutants.

(D) Bioluminescence phenotypes of *V. harveyi* XK006 carrying Kin^{off} *luxN* alleles from our pre-existing collection. For **C** and **D**: white, DMSO; black, 10 μ M 3O-C12 HSL. Error bars represent standard deviations for three replicates.

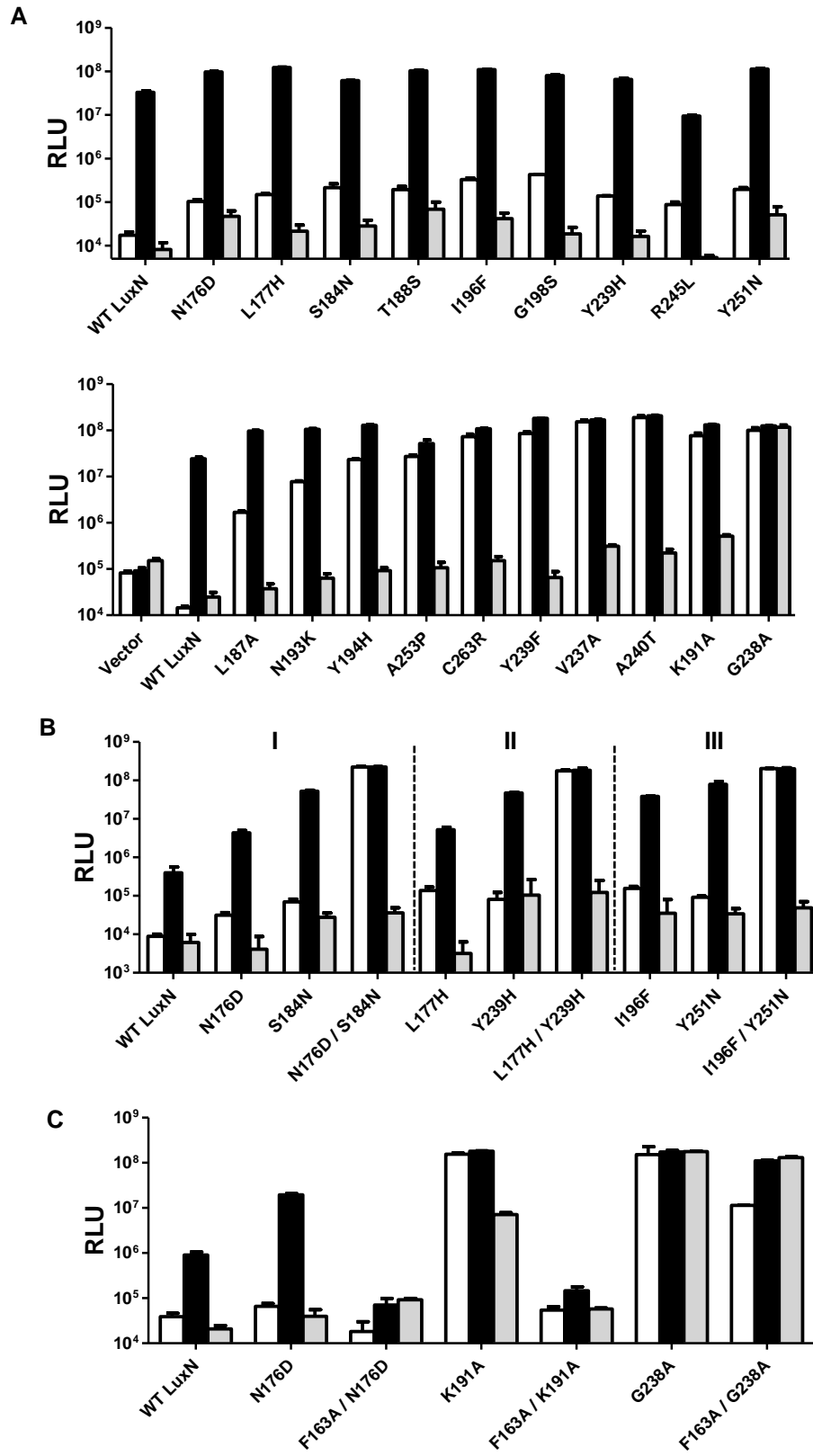


Figure S7

Figure S7. LuxN mutants display a spectrum of biases to the Kin^{off} state.

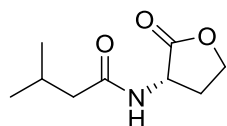
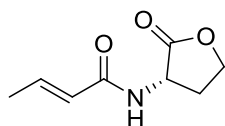
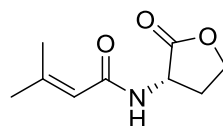
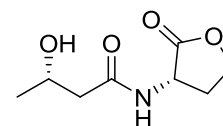
(A) *V. harveyi* XK847 carrying the vector, WT *luxN*, or Kin^{off} *luxN* alleles was assayed for light production in response to the specified AHLs. DMSO, white; 20 nM AI-1, black; 10 μ M 3O-C12 HSL, grey. Error bars represent standard deviations for three replicates. For ease of comparison, alleles are arranged from the one producing least amount of basal light to the one producing the highest basal light going from left to right.

(B) *V. harveyi* XK847 carrying WT *luxN* or Kin^{off} *luxN* alleles was assayed for light production in response to the specified AHLs. Color designations are as in **A**. Single and double mutant combinations are grouped into panels I, II, and III.

(C) *V. harveyi* XK847 carrying WT *luxN*, the Kin^{off} *luxN* alleles, or the various F163A recombinants was assayed for light production in response to the specified AHLs. Color designations are as in **A**. In all panels, error bars represent standard deviations for three replicates.

Table S1. LuxN and LuxN His210 variants' sensitivities to AHLs with different C₃ modifications.

Top: Structures of the synthetic AHLs tested. See also Fig. 1A. Dose-dependent bioluminescence of *V. harveyi* XK006 carrying WT *luxN* or the specified *luxN* alleles was assayed as in Figure 2C. EC₅₀ values are shown as mean ± standard deviation for three replicates; >10⁴ denotes EC₅₀ greater than 10 μM (in these cases, the EC₅₀ could not be reliably determined due to production of less than maximal light at 100 μM); n. r. denotes no response (less than half-maximal induction of light production at 100 μM).

**3Me-C4 HSL****en-C4 HSL****3Me-en-C4 HSL****(S)-3OH-C4 HSL**

HSL	LuxN EC ₅₀ (nM)			
	WT	H210Q	H210N	H210T
(R)-3OH-C4	9 ± 5	43 ± 9	200 ± 80	> 10 ⁴
(S)-3OH-C4	> 10 ⁴	n. r.	1300 ± 300	n. r.
3O-C4	> 10 ⁴	90 ± 30	12 ± 6	1300 ± 300
C4	> 10 ⁴	50 ± 20	22 ± 8	300 ± 80
3Me-C4	5000 ± 2000	200 ± 10	4 ± 1	57 ± 7
en-C4	> 10 ⁴	120 ± 30	18 ± 9	110 ± 76
3Me-en-C4	4800 ± 700	150 ± 30	0.7 ± 0.1	20 ± 10

Table S2. LuxN, LuxN His210, LuxN Leu166 variants' sensitivities to AHLs. Dose-dependent bioluminescence responses to AHLs were measured for *V. harveyi* XK006 carrying WT *luxN* or the specified *luxN* alleles as in Fig. 2C. EC₅₀ values are represented as in Table S1, and the asterisk (*) denotes that the light response plateaued at a submaximal level.

HSL	LuxN EC ₅₀ (nM)			
	WT	L166A	H210N	L166A/ H210N
3OH-C4	9 ± 5	480 ± 30	200 ± 80	> 10 ⁴
3O-C4	> 10 ⁴	n. r.	12 ± 6	1700 ± 700
C4	> 10 ⁴	n. r.	22 ± 8	2100 ± 700
3OH-C6	n. r.	26 ± 6	n. r.	2000 ± 1000*
3O-C6	n. r.	n. r.	900 ± 300*	28 ± 4
C6	n. r.	n. r.	1900 ± 900*	40 ± 20
3OH-C8	n. r.	11 ± 4	n. r.	2700 ± 100*
3O-C8	n. r.	220 ± 80*	n. r.	7 ± 2
C8	n. r.	n. r.	n. r.	32 ± 9
3OH-C10	n. r.	70 ± 30*	n. r.	n. r.
3O-C10	n. r.	n. r.	n. r.	n. r.
C10	n. r.	n. r.	n. r.	n. r.

Table S3. AinR receptors' sensitivities to AHLs. Bioluminescence was measured from *V. harveyi* XK006 harboring WT *ainR* and the specified *ainR* alleles on pFED343 in response to the designated AHLs. EC₅₀ values were calculated from dose-response curves as in Fig. 2C. Notations are as in Table S2.

HSL	AinR EC ₅₀ (nM)				
	WT	Q204H	A160L	S203I	A160L/ S203I
3OH-C4	n. r.	n. r.	n. r.	1500 ± 300	800 ± 400*
3O-C4	n. r.	n. r.	n. r.	n. r.	n. r.
C4	n. r.	n. r.	n. r.	700 ± 400	90 ± 50
3OH-C8	15 ± 7*	n. r.	n. r.	0.4 ± 0.1	n. r.
3O-C8	90 ± 30	n. r.	n. r.	0.8 ± 0.1	n. r.
C8	1.1 ± 0.1	4 ± 1	n. r.	0.3 ± 0.1	n. r.

Table S4. LuxN Kin^{off} receptors' sensitivities to 3O-C12 HSL. Dose-dependent light production from XK847 carrying the specified Kin^{off} *luxN* alleles was measured in response to DMSO and 3O-C12 HSL. Alleles are arranged by increasing EC₅₀ values.

	Kin^{off} LuxN IC₅₀ (nM)					
	C263R	Y239F	V237A	K191A	A240T	G238A
DMSO	n. r.	n. r.	n. r.	n. r.	n. r.	n. r.
3O-C12 HSL	15	55	380	440	640	n. r.

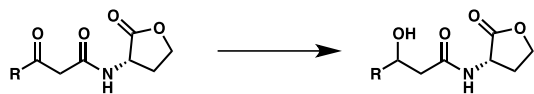
Supplementary Experimental Procedures

Chemical materials and methods

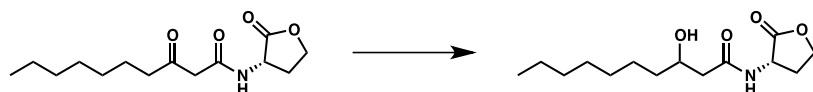
Unless otherwise stated, reactions were performed in flame-dried glassware fitted with rubber septa under a nitrogen atmosphere and were stirred with Teflon-coated magnetic stirring bars. Liquid reagents and solvents were transferred via syringe using standard Schlenk techniques. Reaction solvents were dried by passage over a column of activated alumina. All other solvents and reagents were used as received unless otherwise noted. Reaction temperatures above 23 °C refer to oil bath temperature, which was controlled by an OptiCHEM temperature modulator. Thin layer chromatography was performed using SiliCycle silica gel 60 F-254 precoated plates (0.25 mm) and visualized by UV irradiation and anisaldehyde or potassium permanganate stain. Sorbent standard silica gel (particle size 40-63 μm) was used for flash chromatography. ^1H and ^{13}C NMR spectra were recorded on Bruker Avance III (500 MHz for ^1H ; 125 MHz for ^{13}C) spectrometer fitted with either a ^1H -optimized TCI (H/C/N) cryoprobe or a ^{13}C -optimized dual C/H cryoprobe or a Bruker NanoBay (300 MHz). Chemical shifts (δ) are reported in ppm relative to the residual solvent signal ($\delta = 7.26$ for ^1H NMR and $\delta = 77.0$ for ^{13}C NMR for CDCl_3). Data for ^1H NMR spectra are reported as follows: chemical shift (multiplicity, coupling constants, number of hydrogens). Abbreviations are as follows: s (singlet), d (doublet), t (triplet), dd (doublet of doublets), dq (doublet of quartets), m (multiplet). High-resolution mass spectral analysis was performed using an Agilent 1200-series electrospray ionization – time-of-flight (ESI-TOF) mass spectrometer in the positive ESI mode.

3OH-C4 HSL, C4 HSL, C8 HSL, C10 HSL, C12 HSL 3OH C12-HSL, 3O-C6 HSL, 3O-C8 HSL, 3O-C10 HSL, 3O-C12 HSL are commercially available (Sigma-Aldrich and Cayman Chemical). The syntheses of C6 HSL (Hodgkinson *et al.*, 2011), 3O-C4-HSL (Bycroft *et al.*, 1992), CL (Swem *et al.*, 2009), and PTL (Swem *et al.*, 2009) have been previously reported.

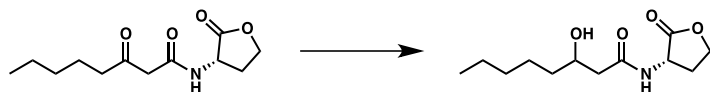
General Procedure A



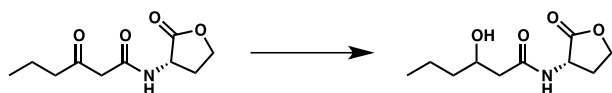
Reduction of β -keto-amide: The 3O-acyl homoserine lactone (1 equiv) was dissolved in anhydrous methanol (0.09 M). A solution of 1.0 M HCl in anhydrous methanol was freshly prepared using acetyl chloride. The reaction mixture was cooled to 0 °C and acidified to pH 3 with the 1.0 M HCl solution. Sodium borohydride was slowly added (1.4 equiv). The pH was adjusted to pH 3 with the 1.0 M HCl solution. The reaction was then stirred for 30 min at 0 °C and concentrated. The crude product was purified by column chromatography.



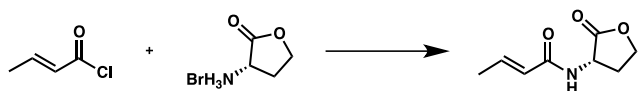
3OH-C10 HSL: 3OH-C10 HSL was synthesized in a 11% yield following general procedure A. **HRMS** (ESI-TOF) calculated for $C_{14}H_{26}NO_4$ $[M+H]^+$: m/z 272.1862, found 272.1844; **1H NMR** (500 MHz, $CDCl_3$) δ 6.57-6.43 (m, 1H), 4.62-4.53 (m, 1H), 4.49 (t, $J = 9.1$ Hz, 1H), 4.34-4.25 (m, 1H), 4.06-3.98 (m, 1H), 2.89-2.79 (m, 1H), 2.50-2.30 (m, 2H), 2.25-2.12 (m, 1H), 1.59-1.19 (m, 12H), 0.88 (t, $J = 6.9$ Hz, 3H); **^{13}C NMR** (125 MHz, $CDCl_3$) δ 175.4, 173.0, 68.6, 66.3, 49.3, 36.9, 31.8, 30.4, 29.4, 29.2, 25.5, 22.6, 14.1.



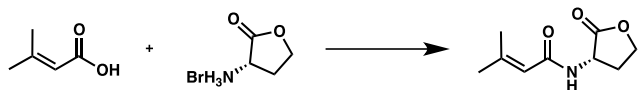
3OH-C8 HSL: 3OH-C8 HSL was synthesized in a 59% yield following general procedure A. **HRMS** (ESI-TOF) calculated for $C_{12}H_{22}NO_4$ $[M+H]^+$: m/z 244.1549, found 244.1525; **1H NMR** (500 MHz, $CDCl_3$) δ 6.58-6.41 (m, 1H), 4.64-4.53 (m, 1H), 4.49 (t, $J = 9.1$ Hz, 1H), 4.34-4.24 (m, 1H), 4.13-3.97 (m, 1H), 3.14-3.02 (m, 1H), 2.88-2.76 (m, 1H), 2.53-2.40 (m, 1H), 2.40-2.30 (m, 1H), 2.26-2.10 (m, 1H), 1.62-1.24 (m, 8H), 0.89 (t, $J = 6.8$ Hz, 3H); **^{13}C NMR** (125 MHz, $CDCl_3$) δ 175.4, 173.0, 68.6, 66.1, 49.2, 42.4, 36.9, 31.6, 30.2, 25.1, 22.6, 14.0.



3OH-C6 HSL: 3OH-C6 HSL was synthesized in a 3% yield following general procedure A. **HRMS** (ESI-TOF) calculated for $C_{10}H_{18}NO_4$ $[M+H]^+$: m/z 216.1236, found 216.1240. **1H NMR** (500 MHz, $CDCl_3$) δ 6.49 (d, $J = 36.1$ Hz, 1H), 4.62-4.52 (m, 1H), 4.49 (t, $J = 9.1$ Hz, 1H), 4.34-4.24 (m, 1H), 4.04 (s, 1H), 3.12-3.01 (m, 1H), 2.89-2.78 (m, 1H), 2.52-2.29 (m, 2H), 2.26-2.11 (m, 1H), 1.55-1.33 (m, 4H), 0.94 (t, $J = 7.0$ Hz, 3H). **^{13}C NMR** (125 MHz, $CDCl_3$) δ 175.3, 173.0, 68.3, 66.1, 49.2, 42.4, 38.9, 30.3, 18.6, 13.9.

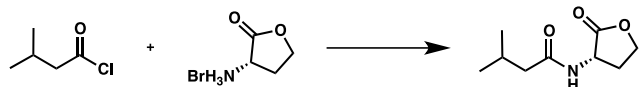


en-C4 HSL: en-C4 HSL was synthesized following the method of (Hodgkinson *et al.*, 2011). L-Homoserine lactone hydrobromide (50 mg, 0.27 mmol, 1.0 equiv) and sodium carbonate (75 mg, 0.71 mmol, 2.6 equiv) were combined in 1:1 CH_2Cl_2/H_2O (2.8 mL). Crotonoyl chloride (0.035 mL, 0.37 mmol, 1.4 equiv) was added dropwise. The reaction was stirred vigorously for 2 h. The layers were separated, and the aqueous phase was extracted with CH_2Cl_2 (2 x 3 mL). The combined organic layer was washed sequentially with saturated aqueous $NaHCO_3$ (2 x 3 mL) and brine (1 x 3 mL). The solution was dried over Na_2SO_4 and concentrated to provide en-C4-HSL in a 21% yield. No further purification was necessary. **HRMS** (ESI-TOF) calculated for $C_8H_{12}NO_3$ $[M+H]^+$: m/z 170.0817, found 170.0815; **1H NMR** (500 MHz, $CDCl_3$) δ 6.92 (dq, $J = 13.8, 6.9$ Hz, 1H), 5.92 (s, 1H), 5.85 (dd, $J = 15.2, 1.6$ Hz, 1H), 4.64-4.55 (m, 1H), 4.49 (t, $J = 9.0$ Hz, 1H), 4.35-4.26 (m, 1H), 2.96-2.86 (m, 1H), 2.23-2.10 (m, 1H), 1.88 (dd, $J = 6.9, 1.6$ Hz, 3H); **^{13}C NMR** (125 MHz, $CDCl_3$) δ 175.5, 166.2, 142.0, 123.7, 66.2, 49.4, 30.8, 17.9.

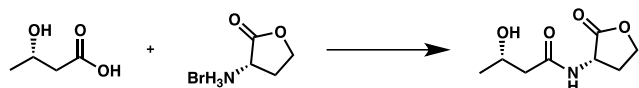


3Me-en-C4 HSL: Homoserine lactone hydrobromide (0.10 g, 0.55 mmol, 1.0 equiv), 3,3-dimethylacrylic acid (55 mg, 0.55 mmol, 1.0 equiv), HOBT (20 mg, 0.15 mmol, 0.27 equiv), EDC (0.12 g, 0.60 mmol, 1.1 equiv), and triethylamine (0.20 mL, 1.4 mmol, 2.5 equiv) were dissolved in 5.5 mL CH_2Cl_2 . After stirring at room temperature for 23 h, the reaction was quenched with H_2O (6 mL). The aqueous layer was extracted with EtOAc (3 x 8 mL). The combined organic layers were washed sequentially with 1 M $NaHSO_4$ (10 mL), saturated $NaHCO_3$ (10 mL) and brine (10 mL). The solution was dried over Na_2SO_4

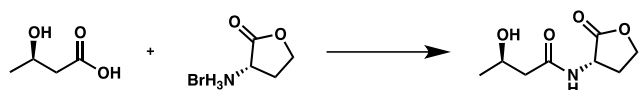
and concentrated. Column chromatography provided 3Me-en-C4-HSL in a 77% yield. **HRMS** (ESI-TOF) calculated for $C_9H_{14}NO_3$ $[M+H]^+$: m/z 184.0973, found 184.0943. **1H NMR** (500 MHz, $CDCl_3$) δ 6.00 (s, 1H), 5.61 (s, 1H), 4.66-4.53 (m, 1H), 4.48 (t, $J = 9.0$ Hz, 1H), 4.34-4.24 (m, 1H), 2.91-2.76 (m, 1H), 2.23-2.11 (m, 4H), 1.86 (s, 3H). **^{13}C NMR** (125 MHz, $CDCl_3$) δ 175.8, 167.1, 153.8, 117.0, 66.1, 49.0, 30.6, 27.4, 19.9.



3Me-C4 HSL: 3Me-C4 HSL was prepared using the same procedure as for en-C4-HSL, starting with isovaleryl chloride. The product was isolated in a 90% yield. **HRMS** (ESI-TOF) calculated for $C_9H_{16}NO_3$ $[M+H]^+$: m/z 186.1130, found 186.1136. **1H NMR** (500 MHz, $CDCl_3$) δ 5.92 (s, 1H), 4.59-4.44 (m, 2H), 4.35-4.24 (m, 1H), 2.97-2.83 (m, 1H), 2.19-2.05 (m, 4H), 0.97 (t, $J = 5.8$ Hz, 6H). **^{13}C NMR** (125 MHz, $CDCl_3$) δ 175.4, 173.1, 66.1, 49.3, 45.4, 30.7, 26.1, 22.4, 22.4.



(S)-3OH-C4 HSL: (S)-3-hydroxybutyric acid (0.29 g, 2.7 mmol, 1.0 equiv), homoserine lactone hydrobromide (0.50 g, 2.7 mmol, 1.0 equiv), and triethylamine (1.2 mL, 8.2 mmol, 3.0 equiv) were dissolved in CH_2Cl_2 (6 mL). BOP-Cl was then added (0.71 g, 2.8 mmol, 1.0 equiv). The reaction was stirred at room temperature for 24 h. The reaction mixture was loaded directly on a silica plug, and was eluted with EtOAc. The product was isolated in a 66% yield. **1H NMR** (500 MHz, $CDCl_3$) δ 6.61-6.42 (m, 1H), 4.67-4.53 (m, 1H), 4.49 (t, $J = 9.0$ Hz, 1H), 4.37-4.25 (m, 1H), 4.25-4.18 (m, 1H), 3.25-3.16 (m, 1H), 2.90-2.77 (m, 1H), 2.49-2.32 (m, 2H), 2.25-2.10 (m, 1H), 1.25 (d, $J = 6.2$ Hz, 3H); **^{13}C NMR** (125 MHz, $CDCl_3$) δ 175.3, 172.8, 66.1, 64.8, 49.1, 43.8, 30.3, 22.9.



(R)-3OH-C4 HSL (AI-1): (R)-3OH-C4 HSL was synthesized using the same procedure as for (S)-3OH-C4 HSL, but starting with (R)-3-hydroxybutyric acid. The product was furnished in a 45% yield. **1H NMR**

(500 MHz, CDCl₃) δ 6.44 (s, 1H), 4.67-4.52 (m, 1H), 4.52-4.45 (m, 1H), 4.36-4.24 (m, 1H), 4.24- 4.18 (m, 1H), 3.16 (d, *J* = 3.5 Hz, 1H), 2.91-2.78 (m, 1H), 2.46 (dd, *J* = 15.5, 2.8 Hz, 1H), 2.35 (dd, *J* = 15.5, 8.9 Hz, 1H), 2.25-2.12 (m, 1H), 1.26 (d, *J* = 6.3 Hz, 3H); ¹³C NMR (125 MHz, CDCl₃) δ 175.2, 172.8, 66.1, 64.7, 49.2, 43.7, 30.3, 22.8.

Supplementary References

Bycroft, B.W., Williams, P., Stewart, G.S.A., Chhabra, S.R., Stead, P., Winson, M.K., *et al.* (1992) Bacterial quorum sensing autoinducers. WO 92018614 A1, Oct. 29.

Hodgkinson, J.T., Galloway, W.R.J.D., Casoli, M., Keane, H., Su, X., Salmond, G.P.C., *et al.* (2011) Robust routes for the synthesis of *N*-acylated-L-homoserine lactone (AHL) quorum sensing molecules with high levels of enantiomeric purity. *Tetrahedron Lett* **52**: 3291–3294.

Swem, L.R., Swem, D.L., O'Loughlin, C.T., Gatmaitan, R., Zhao, B., Ulrich, S.M., and Bassler, B.L. (2009) A quorum-sensing antagonist targets both membrane-bound and cytoplasmic receptors and controls bacterial pathogenicity. *Mol Cell* **35**: 143–53.

¹H NMR Spectra

